Check for updates

Research Article

Modeling Combined Anti-Inflammatory Effects of Dexamethasone and Tofacitinib in Arthritic Rats

Ruihong Yu,[1] Dawei Song,[2] Debra C DuBois,[2,3] Richard R. Almon,[2,3] and William J. Jusko[2,4]

Abstract. Tofacitinib (TOF), a Janus kinase (JAK) inhibitor, which was approved in 2012, has been recommended for the treatment of clinically active rheumatoid arthritis (RA). Dexamethasone (DEX), a potent corticosteroid, is also used in RA therapy but with limited usefulness due to dose- and time-dependent adverse effects. This pilot study examines the single and combined effects of DEX and TOF in order to explore the steroid-sparing potential of TOF. Collagen-induced arthritic (CIA) rats were subcutaneously (SC) dosed with vehicle, 1.5 mg/kg TOF, 5 mg/kg TOF, 0.225 mg/kg DEX, or a combination of 1.5 mg/kg TOF and 0.225 mg/kg DEX. Paw sizes were measured as an index of disease and drug efficacy and dynamically depicted using a logistic function for natural paw growth, a turnover model for disease progression, an indirect response model for inhibitory effects of TOF and DEX and a non-competitive interaction model for the combined effect of DEX and TOF. TOF alone exerted only a slight inhibitory effect on RA paw edema compared to DEX, which reduced edema by 40%. In combination, TOF and DEX had additive effects with an interaction factor of 0.76. Using model simulations, a single SC dose of TOF does not have a visible steroid-sparing potential, although BID oral dosing has such potential. The current study suggests an additive effect of TOF and DEX and simulations indicate that further exploration of TOF and DEX administration timing may produce desirable drug efficacy with lower DEX doses.

KEY WORDS: anti-inflammatory; collagen-induced arthritis; dexamethasone; steroid-sparing; tofacitinib.

INTRODUCTION

Rheumatoid arthritis (RA) is one of the most prevalent chronic inflammatory and autoimmune diseases (1). This disease involves continuous synovitis along with systemic and local levels of inflammation and autoantibody production. Clinically, RA results in pain, swelling and stiffness of joints, followed by cartilage destruction and bone erosion, as well as deformity and dysfunction (1). Currently available drugs for RA treatment include corticosteroids (CS), nonsteroidal anti-inflammatory drugs (NSAIDs) and a number of disease-modifying antirheumatic drugs (DMARDs) (2). The DMARDs are further classified into conventional synthetic, targeted synthetic and biological DMARDs, of which representative agents include methotrexate, tofacitinib (TOF) and infliximab for these categories (2,3).

As a synthetic corticosteroid, dexamethasone (DEX) can exhibit potent immune suppression and alleviate disease symptoms in RA. It binds to cytosolic glucocorticoid receptors, inhibiting nuclear factor NF-κB signaling, the mitogen-activated protein kinase (MAPK) pathway and downstream activator protein-1 (AP-1), thus suppressing the production of multiple pro-inflammatory mediators such as interleukin-1β and tumor necrosis factor-α and exerting anti-inflammatory and immuno-suppressive effects (4,5). In addition, its rapid inhibitory action towards inflammation may relate to non-genomic mechanisms (6). Due to the chronic and refractory nature of RA, steroid therapy may require chronic treatment in order to maintain the suppression of immunological functions. However, adverse effects associated with long-term use, such as infections and osteoporosis, have negative influences on quality of life.

A recent approach to RA treatment involves JAK inhibitors that function through inhibition of the Janus kinase (JAK)-signal transducers and activators of transcription

Ruihong Yu and Dawei Song contributed equally to this work.

[1] Department of Pharmacology, School of Basic Medical Sciences, Xi'an Jiaotong University Health Science Center, Xi'an, 710061, China.
[2] Department of Pharmaceutical Sciences, School of Pharmacy and Pharmaceutical Sciences, State University of New York at Buffalo, 404 Pharmacy Building, Buffalo, NY 14214-8033, USA.
[3] Department of Biological Sciences, State University of New York at Buffalo, Buffalo, NY 14260, USA.
[4] To whom correspondence should be addressed. (e–mail: wjjusko@buffalo.edu)

aaps®

(STAT) pathways that play an important role in signaling transduction of cytokines involved in the pathogenesis of RA [7,8]. Additionally, TOF, the first drug approved in the JAK inhibitor family, has demonstrated potent efficacy in mouse and rat arthritis models, including paw swelling relief, decrease of inflammatory biomarkers [9], and diminished structural damage of arthritic joints [10,11].

Combination therapy is a common strategy for the treatment of rheumatoid arthritis in order to achieve better therapeutic outcomes [3]. Based on the pharmacological mechanisms of TOF and DEX, combined administration of the two drugs may achieve better therapeutic effects by interfering with proinflammatory cytokine signal transduction through inhibition of their corresponding signaling pathways. This study assessed the efficacy of DEX and TOF in the rat CIA model in order to determine whether there is a synergistic effect on suppression of inflammation and explores the possible steroid-sparing potential of TOF.

MATERIALS AND METHODS

Reagents and Chemicals

Tofacitinib citrate salt was purchased from LC Laboratories (Woburn, MA). Dexamethasone sodium phosphate solution (pharmaceutical grade) was purchased from Bimeda Pharmaceuticals (Dublin, Ireland). Type II porcine collagen was supplied by Chondrex Inc. (Redmond, WA). Incomplete Freund's adjuvant (IFA) and all other chemicals were purchased from Sigma-Aldrich (St Louis, MO).

Animals

Male Lewis rats ($n = 26$), weighing around 120 g were purchased at 5–6 weeks of age from Envigo (Indianapolis, IN). All rats were housed individually with free access to food and water in the University Laboratory Animal Facility under controlled environmental conditions. Animals were acclimated for 1 week before experiments. The research protocol adhered to the *Guide for the Care and Use of Laboratory Animals* (National Research Council, 2011) and was approved by the University at Buffalo Institutional Animal Care and Use Committee.

Experimental Procedures

Hind paw swelling was evaluated by the total cross-sectional areas of the forefoot and the ankle measured by digital calipers (VWR Scientific, Rochester, NY). Arthritis was induced using porcine collagen emulsified in Incomplete Freunds Adjuvant and injected intradermally, with a booster injection given 7 days later, as described in a previous publication [12]. Our previous studies involving CIA induction showed that the paw edema peak occurs on day 21 for male rats [13]. Paw measurements therefore were carried out on days 0, 3, 7, 9, 11, 13, 15, 17, 19, and 20 post-induction. Based on day 20 measurements, 19 rats with at least a 50% increase in at least one hind paw were included for treatment on day 21 and randomly assigned to one of five groups ($n = 3\sim4$): vehicle, 1.5 mg/kg TOF, 5.0 mg/kg TOF, 0.225 mg/kg DEX, and 0.225 mg/kg DEX combined with 1.5 mg/kg TOF.

The drugs were injected subcutaneously in volumes of 1 mL/kg at the nape of the neck on day 21, and paw edema was further measured at 0, 1, 2, 4, 6, 8, 12, 24, 36, 48, 96, and 144 h post-dosing. The DEX dosing solution was freshly prepared by directly diluting the dexamethasone sodium phosphate solution with phosphate-buffered saline. The TOF dosing solution was freshly prepared by dissolving TOF citrate salt into 33.3% DMSO/66.6% PEG300. Paw measurements were also performed on 7 rats without any observable paw edema after induction and assigned as non-CIA controls in order to assess their natural growth.

PK/PD Models

TOF PK Modeling and Simulation

There were 9 sets of TOF mean plasma concentration versus time data from three species digitized with GSYS 2.4 (Hokkaido University Nuclear Reaction Data Center, Sapporo, Japan). Doses were 25 mg/kg IV and 5 mg/kg PO from Kumar *et al.* [14] and 5 mg/kg IV and 1 mg/kg PO from Sharma *et al.* [15] in healthy male Sprague-Dawley rats. Also, 2 mg/kg IV and 10 mg/kg PO from Dixit *et al.* [16] in male Balb/C mice and 50 mg PO from Dowty *et al.* [17] and 30 and 100 mg PO from Krishnaswami *et al.* [18] in healthy adult volunteers.

The PK of TOF was depicted with a basic minimal physiologically based pharmacokinetic (mPBPK) model with two tissue compartments [19] (Fig. 1). Tissues are divided into two compartments, V_{RPT} and V_{SPT} according to their blood perfusion characteristics. Muscle, skin, and adipose are assigned as slowly perfused tissue (SPT), whereas liver, kidney, heart, and all other tissues are denoted as rapidly perfused tissue (RPT). The model equations and initial conditions are:

$$\frac{dC_b}{dt} = \frac{Input}{V_b} + \frac{\left[f_{d,RPT} \cdot Q_{co} \cdot \left(\frac{C_{RPT}}{K_{p,RPT}} - C_b\right) + f_{d,SPT} \cdot Q_{co} \cdot \left(\frac{C_{SPT}}{K_{p,SPT}} - C_b\right) - CL \cdot C_b\right]}{V_b}, \quad C_b(0) = 0 \quad (1)$$

$$\frac{dC_{RPT}}{dt} = \left[f_{d,RPT} \cdot Q_{co} \cdot \left(C_b - \frac{C_{RPT}}{K_{p,RPT}}\right)\right] / V_{RPT}, \qquad C_{RPT}(0) = 0 \quad (2)$$

$$\frac{dC_{SPT}}{dt} = \left[f_{d,SPT} \cdot Q_{co} \cdot \left(C_b - \frac{C_{SPT}}{K_{p,SPT}}\right)\right] / V_{SPT}, \qquad C_{SPT}(0) = 0 \quad (3)$$

where *Input* is the drug amount entering into blood, which equals to *Dose* or $k_{a,po} \cdot Dose / F_{po}$ for IV and PO administration ($k_{a,po}$ and F_{po} indicate first-order oral absorption rate constant and bioavailability), C_b is the total concentration of TOF in V_b (blood volume), C_{RPT} and C_{SPT} are the total TOF concentration in V_{RPT} and V_{SPT}, Q_{co} is cardiac output of each species, $f_{d,RPT}$ and $f_{d,SPT}$ are the fraction of TOF in Q_{co} accessing V_{RPT} and V_{SPT}, $K_{p,RPT}$ and $K_{p,SPT}$ are the tissue/plasma partition coefficient of TOF in RPT and SPT, and *CL* is the systemic clearance of TOF.

The physiological parameters, V_b, V_{RPT}, V_{SPT}, $f_{d,RPT}$, $f_{d,SPT}$, and Q_{co}, were obtained from Davies and Morris (20), Kawai *et al.* (21), and Shah and Betts (22). The digitized TOF PK data sets were simultaneously fitted across all doses and species. The $k_{a,po}$ was estimated by individually fitting within species, F_{po} was obtained directly from or calculated based on the original studies. Some physiological restrictions of relevant parameters are $f_{d,RPT} + f_{d,SPT} = 1$ and $V_b + V_{RPT} + V_{SPT} = $ BW. The $K_{p,RPT}$ and $K_{p,SPT}$ values were assumed consistent among all species, and CL was allometrically scaled as a function of body weight (BW):

$$CL = a \cdot BW^b \qquad (4)$$

where a is the allometric coefficient, b is the allometric exponent, and BW is the reported body weights with kilogram unit (kg).

Based on the estimated PK parameters of TOF, this mPBPK model was then used to simulate the blood and tissue concentrations of TOF in CIA rats subcutaneously (SC) receiving 1.5 and 5.0 mg/kg TOF with SC-specific parameters, $k_{a,sc}$ and F_{sc}.

The assumptions for the PK simulation of SC dosing TOF were the following: The first-order absorption rate constant of TOF following SC dosing ($k_{a,sc}$) is the same as DEX. The SC bioavailability of TOF ($F_{sc,T}$) is 100%. No differences in TOF PK exist between Sprague-Dawley and Lewis rats or between healthy and CIA rats.

DEX PK Simulation

The mPBPK model with one tissue compartment shown in Fig. 1 was applied to simulate the DEX concentration in CIA rats, and the corresponding PK parameters were described by Song *et al.* (13).

PD Model

The PD model scheme presented in Fig. 1 was used to characterize disease progression of CIA rats and the anti-inflammatory effects of DEX and TOF. A logistic growth function was applied to describe the natural growth of the paw according to Li *et al.* (24).

The paw size change over time and initial condition for all healthy controls and CIA rats before disease onset were described as:

$$\frac{dPaw}{dt} = k_g \cdot Paw \cdot \left(1 - \frac{Paw}{Paw_{ss}}\right), t < t_{onset}, \quad Paw(0) = Paw_0 \quad (5)$$

where *Paw* is the sum cross-sectional areas of the forefoot and ankle of rat hindfoot, Paw_{ss} is the steady-state paw size observed in natural growth, Paw_0 is the initial paw size at CIA induction, k_g is the natural first-order growth rate constant of paws in healthy rats, and t_{onset} is the time when paw edema began.
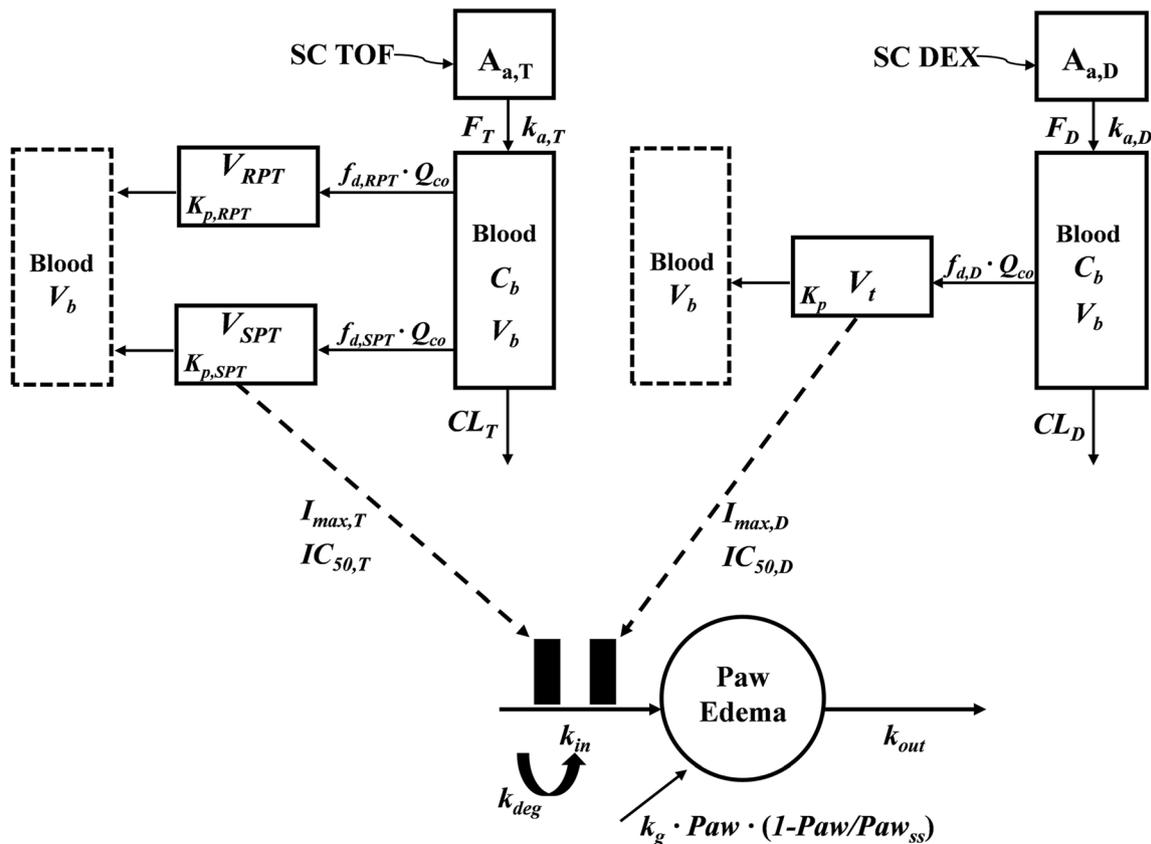

Fig. 1. Schematic of the PK/PD/DIS progression model for effects of DEX and/or TOF on paw edema in CIA rats. Symbols are defined in Table I and II

After disease onset, a turnover model was applied to characterize the disease progression with changes of paw size without treatment over time described as:

$$\frac{dPaw}{dt} = k_g \cdot Paw \cdot \left(1 - \frac{Paw}{Paw_{ss}}\right) + k_{in}(t) - k_{out} \cdot Paw, \quad t \geq t_{onset} \quad Paw(0) = Paw_0 \quad (6)$$

$$\frac{dk_{in}}{dt} = -k_{deg} \cdot k_{in}, \qquad\qquad k_{in}(0) = k_{in0} \qquad (7)$$

where $k_{in}(t)$ indicates the varying production rate of paw edema over time, k_{out} is the first-order rate constant of paw edema dissipation, and k_{deg} is the first-order rate constant of k_{in} decline resulting from the natural remission of paw edema.

The single drug (TOF or DEX) effects on the paw edema of CIA rats were characterized with an indirect response model (IDR) to address their individual inhibitory effect on the production of paw edema (25).

$$\frac{dPaw}{dt} = k_g \cdot Paw \cdot \left(1 - \frac{Paw}{Paw_{ss}}\right) + k_{in}(t) \cdot \left(1 - \frac{I_{max} \cdot C}{IC_{50} + C}\right) - k_{out} \cdot Paw, \quad t \geq t_{onset}$$

$$Paw(0) = Paw_0 \quad (8)$$

where I_{max} ($I_{max,D}$, $I_{max,T}$) refers to the maximum inhibitory effect of DEX or TOF on the production of paw edema, IC_{50} ($IC_{50,D}$, $IC_{50,T}$) is the corresponding drug concentration of the effect site required for 50% of maximal effect.

The model assumed that the unbound TOF concentrations in the SPT compartment ($C_{uSPT,T}$) drive the anti-inflammatory effects of TOF, whereas the unbound DEX concentration of the only tissue compartment ($C_{ut,D}$) drives DEX PD. The unbound drug concentrations in corresponding compartments were calculated as the total concentration times the unbound fraction in tissue ($f_{ut,D}$ or $f_{uSPT,T}$) with the latter calculated as:

$$f_{ut,D} = \frac{f_{up,D}}{K_{p,D}} \text{ and } f_{uSPT,T} = \frac{f_{up,T}}{K_{p,SPT,T}}$$

where the unbound fraction of DEX in plasma ($f_{up,D}$) is 0.3 (24) and that of TOF ($f_{up,T}$) is 0.85. The tissue/plasma partition coefficient of DEX ($K_{p,D}$) is 0.63 (24).

For the TOF and DEX combination group, the IDR model with non-competitive functional interaction was applied to describe paw sizes (24,26).

$$\frac{dPaw}{dt} = k_g \cdot Paw \cdot \left(1 - \frac{Paw}{Paw_{ss}}\right) + k_{in}(t) \cdot \left(1 - \frac{I_{max,T} \cdot C_{uSPT,T}}{IC_{50,T} + C_{uSPT,T}}\right) \cdot$$
$$\left(1 - \frac{I_{max,D} \cdot C_{ut,D}}{\psi \cdot IC_{50,D} + C_{ut,D}}\right) - k_{out} \cdot Paw, \quad t \geq t_{onset} \quad Paw(0) = Paw_0$$

$$(9)$$

where ψ is the interaction term applied to assess the effect of TOF on the pharmacodynamics of DEX as a change in the associated IC value.

Model Fitting

The PK parameters of DEX and TOF obtained from PK modeling were fixed in the subsequent PD analysis. Both the across-species PK fitting for TOF and the PD fittings for the paw sizes were conducted simultaneously among all groups. All fittings and simulations were implemented using ADAPT 5 (Biomedical Simulations Resource, Los Angeles, CA) (27) using maximum likelihood estimation. The model was evaluated

based on goodness-of-fit criteria including Akaike Information Criterion (AIC), visual inspection of the fitted profiles, and CV% of parameter estimates. The variance model was set as:

$$V_i = (\sigma_1 + \sigma_2 \cdot Y_i)^2 \qquad (10)$$

where V_i represents the variance of the ith data point, Y_i is the ith model prediction, and σ_1 as well as σ_2 are the variance model parameters. All figures were created using GraphPad Prism 7.04 (GraphPad Software, La Jolla, CA).

RESULTS

Pharmacokinetics of TOF in CIA Rats

The joint PK fitting profiles of TOF among rat, mice, and human using a basic mPBPK model with allometric scaled CL
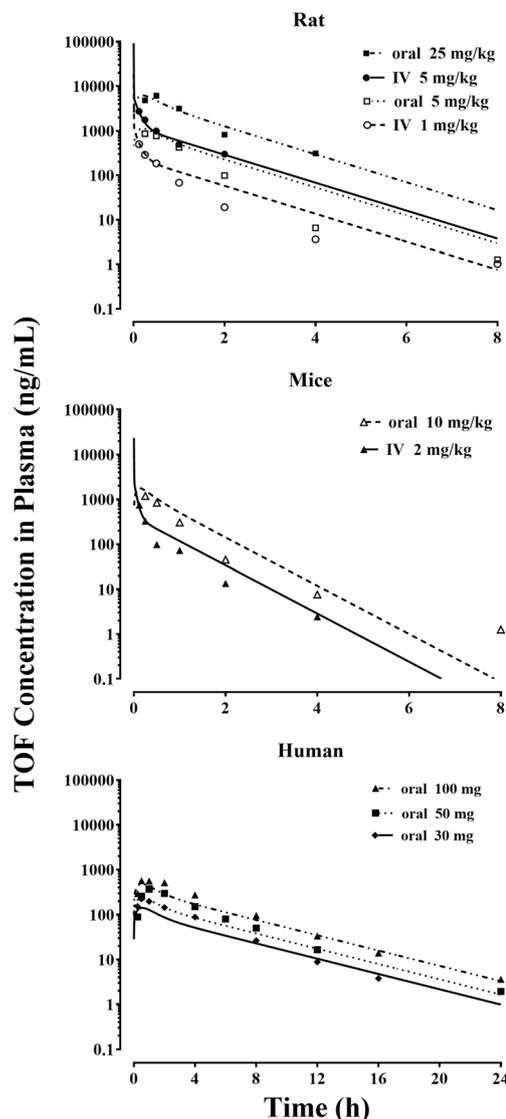

Fig. 2. Digitized mean TOF concentration-time data following the indicated doses in healthy rats, mice, and humans and their jointly fitting profiles across species based on the mPBPK model (Fig. 1). Parameters utilized and estimates are listed in Table I

across species are shown in Fig. 2. The arrays of digitized data were well-captured. The resulting PK parameter estimates of TOF have reasonable CV% as listed in Table I. The allometric exponent value of TOF clearance is 0.75, which is a typical value (28,29). The CL prediction of TOF in rats was 2062 mL/h/kg (equals 34.4 mL/min/kg), which is similar to the noncompartmental analyses, 53.2 and 44.8 mL/min/kg, found by Sharma et al. (15) and Kumar et al. (14).

Based on the model assumptions and the estimated parameters of TOF, the simulated TOF concentrations in blood, SPT (including total and unbound concentration), and RPT compartment following the 1.5 and 5.0 mg/kg SC dosing in CIA rats utilized in the current study are presented in Fig. 3. The plasma TOF concentration covers a range up to 500 ng/mL following 1.5 mg/kg dosing and up to 1500 ng/mL with a 5.0 mg/kg dose. Simulations suggest that TOF has higher concentrations in tissues compared to plasma with consistent K_p values of 1.84 and 2.21 in RPT and SPT across species (Table I). The temporal profile of unbound TOF concentrations in the SPT compartment as shown in Fig. 3 was used as the entity exerting anti-inflammatory effects in the PD model.

Single and Combined Effects of TOF and DEX

The PK/PD/disease (DIS) model shown in Fig. 1 was used to characterize the paw size jointly in non-CIA control and treated/untreated CIA rats. The naive pooled observations from both right and left hind paw measurement and corresponding fitted profiles are shown in Fig. 4. The PD parameter estimates listed in Table II indicate that the paw size dynamics in all six groups were captured well with the model.

Before disease onset, the increase of rat paw size followed the logistic growth model with hypothetical paw size at steady-state (Paw_{ss}) was estimated to be 98.6 mm^2, which is comparable to 108 mm^2 found by Song et al. (13) and 103 mm^2 by Li et al. (16) in male CIA rats, and a 0.00103/h paw growth rate constant that is close to 0.001/h from Song et al. (13).

The paw edema in CIA rats initially appeared around day 14 (340 h) post-induction with observable inter-individual variability. The disease progression was described by a turnover model in which disease production rate constant (k_{in0}) at disease onset was 1.69 mm^2/h, loss of edema production rate constant (k_{deg}) was 0.000565/h, and the loss of edema rate constant (k_{out}) was 0.0106/h. The paw edema of male CIA rats peaked at day 21 (504 h) post-induction.

With 0.225 mg/kg DEX, the paw edema was clearly alleviated with an $IC_{50,D}$ of 0.09 ng/mL, which is comparable to 0.015 but less than 0.39 ng/mL found in previous studies (13,24). The paw edema suppression by TOF was less effective. The I_{max} of TOF was 0.61 following the single SC dose, while the unbound TOF concentration in slowly perfused tissues at 50% $I_{max,T}$ ($IC_{50,T}$) was 1.14 ng/mL. The high-dose and low-dose TOF-treated groups did not show distinct dose-dependent suppression of paw edema. The combination of TOF and DEX dosing displayed only additive effects in CIA rats as indicated by the interaction term (ψ), which was estimated to be 0.76 and was not significantly different from 1 as its 95% confidence interval (-0.55, 2.07) overlapped with 1.0.

Simulation of TOF Steroid-Sparing Effect

The PK/PD/DIS model was subsequently used to simulate the single-dose effects of DEX and combination effects of TOF and DEX in male CIA rats. The PD parameters were fixed to the estimates in Table II with the average value of k_{in0} (1.69 mm^2/h) and Paw_0 (68.94 mm^2). As TOF is employed at 5 mg BID oral doses clinically, dual oral doses of TOF were included in the combination assessment with 0.225 mg/kg DEX to predict its potential steroid-sparing effect. Figure 5 demonstrates that the combination dosage regimen, 0.225 mg/kg SC DEX at 504 h and 2.5 mg/kg oral TOF at 522 and 526 h, may nearly

Table I. Physiological Parameters Used for Allometric Scaling of TOF PK and Corresponding Parameter Estimates (CV%)

Parameters (units)	Definition	Rat (0.25 kg)	Mouse (0.02 kg)	Human (70 kg)
F_{po}	Oral bioavailability	60.9%[a] 67.8%[b]	57.2%[c]	74%[d]
$k_{a,po}$[e] (/h)	Oral absorption rate constant	3.27	3.96	1.36
$f_{d,RPT}$	Fraction of cardiac blood flow accessing rapidly-perfused tissues (RPT)	0.82	0.80	0.77
$f_{d,SPT}$	Fraction of cardiac blood flow accessing slowly-perfused tissues (SPT)	0.18	0.20	0.23
V_b (mL)	Blood volume	13.5	1.7	5200
V_{RPT} (mL)	Volume of lumped rapidly-perfused tissues	64.5	4.0	17,000
V_{SPT} (mL)	Volume of lumped slowly-perfused tissues	172	14.3	47,800
Q_{co} (mL/h)	Cardiac blood flow	4440	480	336,000
$K_{p,RPT}$	Tissue: blood partition coefficient in RPT	1.84 (27.8)		
$K_{p,SPT}$	Tissue: blood partition coefficient in SPT	2.21 (6.8)		
a	Allometric coefficient	1462 (4.5)		
b	Allometric exponent	0.75 (1.5)		
CL (mL/h/kg)	Predicted clearance	2062.4	3860.5	509.4

Physiological parameter values were obtained from Davies and Morris (20), Kawai et al. (21), and Shah and Betts (22)
[a] F_{po} value calculated based on Sharma et al. (15)
[b] F_{po} value calculated based on Kumar et al. (14)
[c] F_{po} value from Dixit et al. (16)
[d] F_{po} value from Gupta et al. (17,23)
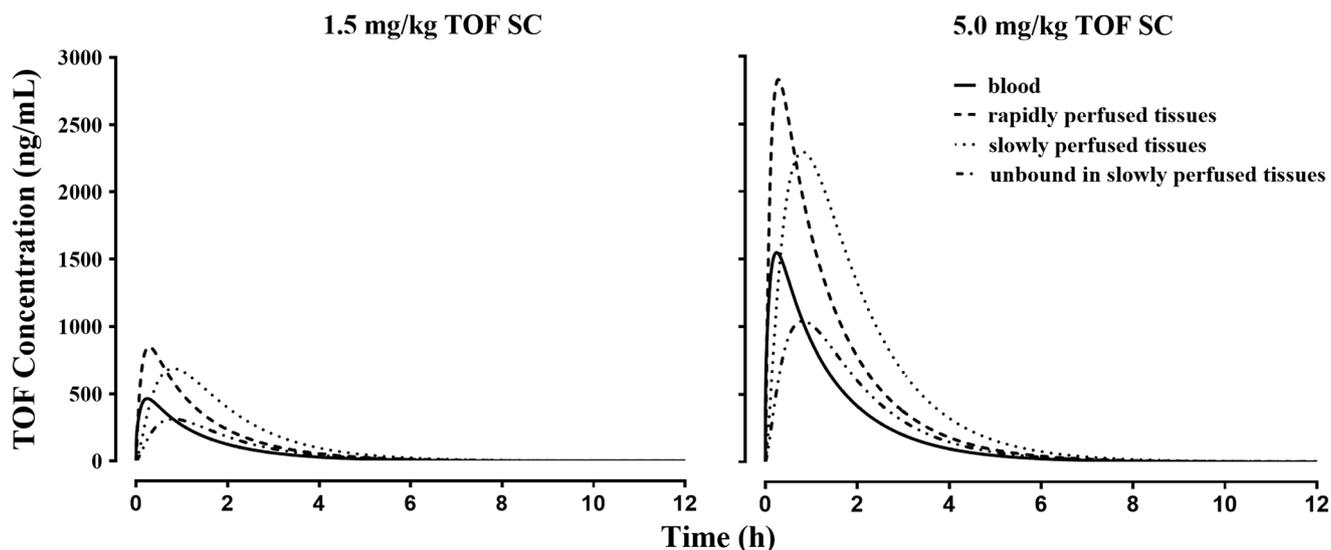[e] $k_{a,po}$ values estimated in preliminary PK fitting within species

Fig. 3. Simulated TOF concentration of blood, rapidly and slowly perfused tissue compartments after 1.5 and 5.0 mg/kg SC dosing in male rats

achieve the same paw edema alleviation exerted by the single dose of 2.25 mg/kg DEX.

DISCUSSION

Corticosteroids, such as DEX, play an important role in rheumatoid arthritis therapy because of their potent anti-inflammatory effect and consequent rapid symptom relief action (6,30). However, the side effects owing to long-term use limit their application, and therefore combination regimens may allow for reduction of their doses without

compromising efficacy. Here, we studied the joint anti-inflammatory effect of DEX and TOF in a pilot study to ascertain whether steroid-sparing occurs.

Our main purpose was to evaluate the PD effects of TOF and DEX utilizing tissue concentrations approximating the site of action as the driving force for pharmacological effects. However, since only plasma PK profiles were available, implementation of a full PBPK model is not feasible and the mPBPK model is an option. Compared to conventional compartmental models, mPBPK models parsimoniously generate physiologically relevant PK parameters that have a
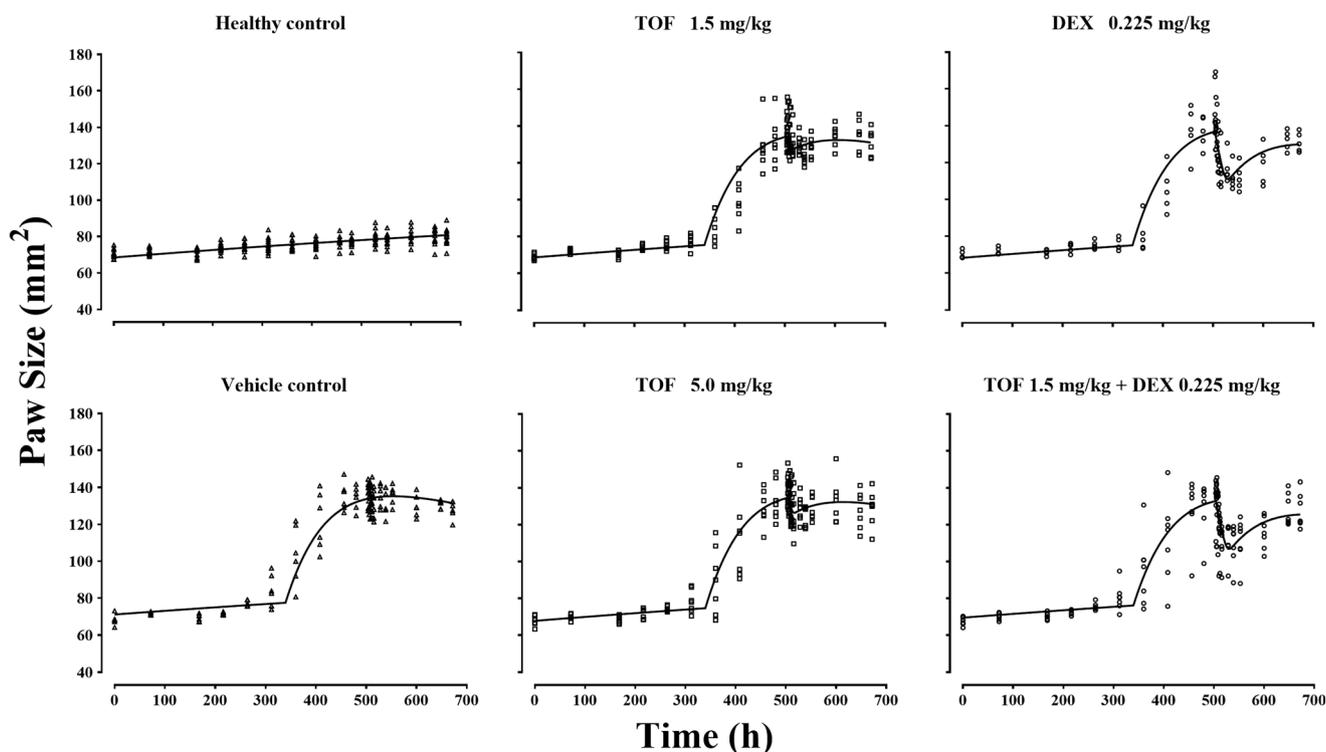

Fig. 4. The paw size versus time profiles of healthy and arthritic rats treated with vehicle and the indicated drug doses. Symbols are measured values and lines are model fittings

Table II. Pharmacodynamic parameter estimates for single and combined effects of DEX and TOF

Parameter (unit)	Definition	Estimates (CV%)
Disease-specific		
t_{onset} (h)	Time of disease onset	339.7 (0.7)
k_g (/h)	Natural growth rate constant	0.00103 (75.7)
k_{out} (/h)	Loss of edema rate constant	0.0106 (14.4)
k_{deg} (/h)	Loss of production rate constant	0.000565 (19.3)
Paw_{ss} (mm^2)	Paw size at steady-state	98.6 (24.5)
$Paw_{0,hC}$ (mm^2)	Paw size on day 0 for healthy controls	68.42 (1.2)
$Paw_{0,vC}$ (mm^2)	Paw size on day 0 for vehicle control group	71.10 (1.5)
$k_{in0,vC}$ (mm^2/h)	Disease production rate constant at t_{onset} for vehicle control group	1.68 (9.1)
$Paw_{0,IT}$ (mm^2)	Paw size on day 0 for 1.5 mg/kg TOF group	68.60 (1.5)
$k_{in0,IT}$ (mm^2/h)	Disease production rate constant at t_{onset} for 1.5 mg/kg TOF group	1.69 (9.0)
$Paw_{0,hT}$ (mm^2)	Paw size on day 0 for 5.0 mg/kg TOF group	67.78 (1.5)
$k_{in0,hT}$ (mm^2/h)	Disease production rate constant at t_{onset} for 5.0 mg/kg TOF group	1.69 (9.0)
$Paw_{0,D}$ (mm^2)	Paw size on day 0 for 0.225 mg/kg DEX group	68.23 (1.7)
$k_{in0,D}$ (mm^2/h)	Disease production constant at t_{onset} for 0.225 mg/kg DEX group	1.73 (9.2)
$Paw_{0,Com}$ (mm^2)	Paw size on day 0 for joint 1.5 mg/kg TOF & 0.225 mg/kg DEX group	69.50 (1.4)
$k_{in0,Com}$ (mm^2/h)	Disease production rate constant at t_{onset} for joint 1.5 mg/kg TOF & 0.225 mg/kg DEX group	1.66 (9.4)
Drug-specific		
$I_{max,T}$	Maximum inhibition of TOF on production of paw edema	0.61 (41.3)
$IC_{50,T}$ (ng/mL)	Unbound tissue concentration of TOF at 50% $I_{max,T}$	1.14 (282.5)
$I_{max,D}$	Maximum inhibition of DEX on production of paw edema	1 (fixed)
$IC_{50,D}$ (ng/mL)	Unbound tissue concentration of DEX at 50% $I_{max,D}$	0.092 (81.4)
Drug interaction parameter		
ψ	Interaction term for inhibition of paw edema production	0.76 (86.2)

mechanistic and logical basis for data interpretation. There have been only two reports of TOF PK in rats with unclear drug absorption rates and no data available in the terminal phase after 8 h post-dosing. Whereas, TOF peak effects appeared at around 10 h post-dosing and thus greater certainty regarding the later concentrations were needed. The allometric scaling model was applied with the addition of PK data from mice and humans to support the rat PK data. The lack of data in the terminal phase may account for the higher *CL* value obtained from noncompartmental analysis in rats than our inter-species scaling predicted value.
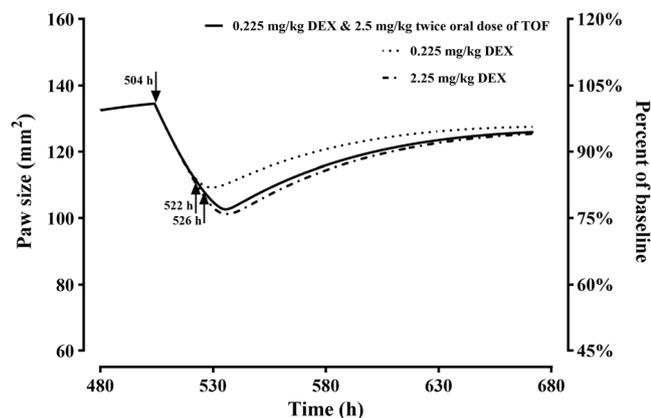

Fig. 5. Model-simulated paw size versus time profiles after 0.225 and 2.25 mg/kg single SC doses of DEX and combined of 0.225 mg/kg SC DEX and 2.5 mg/kg BID oral TOF doses in CIA rats ($\psi = 0.76$). The arrows indicate the time of DEX dosing at 504 h and that of dual TOF dosing at 522 and 526 h

In humans, tofacitinib PK exhibits rapid absorption, rapid elimination, and dose-proportional systemic exposures [18], which were recapitulated in our digitized profiles. Downty et al. [17] reported the time to peak concentration of TOF in humans as ranging 0.3~1.0 h and which was similar in mice [16,17]. The F_{po} of TOF was reported to be 59.4% in rats [15], 57.2% in mice [16] and 74% in humans [17,23], and the $k_{a,po}$ of TOF was preliminarily estimated to be 3.27, 1.36, and 3.96/h in these species. All of the above information suggested that TOF is a well-absorbed drug. Thus, in the simulations of SC TOF doses in rats, we assumed 100% SC bioavailability of TOF and fixed the absorption rate constant to be the same value as DEX due to lack of other relevant information. In man, the primary elimination mechanisms for TOF are renal excretion (circa 30%) and CYP3A4/2C19-mediated hepatic metabolism (circa 70%), with 50 to 55% of overall total clearance attributed to CYP3A4 [17]. Tofacitinib exposures in patients with RA [31] and psoriasis [32] are higher compared to healthy volunteers, and it was hypothesized that this may be attributable to the down-regulation of CYP3A4 activity with inflammation [33]. However, in a previous study, the PK of DEX in male CIA rats was not altered by RA [12] and the metabolism of DEX in male rats is also predominantly CYP3A-mediated [34,35]. Thus, we assumed that TOF PK was not altered by CIA and used the parameters predicted from healthy rats for the PK of TOF in CIA rats. TOF has been reported to lack inhibitive or inductive effects on CYP3A activity and is unlikely to influence the CYP enzyme system [36]. DEX induces CYP3A via PXR gene activation [37] and affects CYP3A-mediated metabolism of lapatinib [38]. However, our study was conducted at a single DEX dose. Therefore, we assume that

co-administration of TOF and DEX will not influence each other's PK behavior. The PK of tofacitinib in CIA rats needs further confirmation.

It can be noted that we previously demonstrated that the mPBPK modeling approach provided reasonable expectations of unbound DEX and naproxen concentrations in rat interstitial fluids (Li *et al.*, 23) and thus we used a similar PK model with two tissue compartments for TOF. The ankle joint in which TOF exerted its anti-inflammatory action is a slowly perfused body part compared with the rapidly perfused tissues and was grouped together with skin, muscle, and adipose into the SPT compartment. Therefore, the unbound TOF concentrations in the SPT space were assigned as the driving force for the alleviation of paw edema.

An indirect response model was used to characterize the effects of DEX and TOF on paw swelling because the drugs interfere with pro-inflammatory cytokine production and disrupt responses such as recruitment of immune effector cells (39). The maximal concentration of TOF in the SPT compartment occurs at 0.75 h after SC dosing, while the peak paw edema suppression was seen around 10 h. Similar time delays between peak concentration and peak drug effect were also seen in DEX-treated CIA rats, which presumably reflects the time needed for cytokine dissipation (k_{out}). Compared with the DEX-treated group, TOF has less potency as indicated by both paw size profiles and the $I_{max,T} = 0.61$. There was little difference in paw edema alleviation between the two doses of TOF. This might be due to the low drug concentrations. The peak biophase TOF concentrations even in the high dose group were far below the $IC_{50,T}$, 1.14 ng/mL. In this study, the one dose of DEX makes it difficult to obtain $I_{max,D}$ during the paw size modeling. However, our previous DEX study (13,24) provided evidence for its potent anti-inflammatory effect in rats with the $I_{max,D}$ value of 1. Thus, continuous administration of TOF by either multiple-dosing or infusion might be better than single dosing for pharmacologic investigation in rats.

Based on paw size profiles, we observed similar paw edema suppression for DEX and combined treatments. This supports the conclusion of additive effects of DEX and TOF. The estimated interaction term, ψ, was around 1 and confirmed an additive effect. Clinically, TOF is recommended as a BID oral dose (40,41) and thus we simulated the combined effects of a BID oral dose regimen of TOF and single SC dose of DEX in CIA rats. Administering two drugs with better timing could achieve the same efficacy as a single drug at high dose, which might indicate that for the drug combination, optimizing dosing time is important. In addition, TOF could help protect bone from resorption caused by either RA or DEX-associated side effects. Bone mineral density could serve as another PD endpoint to fully evaluate the value of this combination regimen.

CONCLUSIONS

The mPBPK and indirect response models well-captured the anti-inflammatory effects of TOF and DEX in CIA rats, and the current DIS and response profiles can serve as a guide for designing further preclinical TOF or other JAK inhibitor studies utilizing CIA rats. A single SC dose of TOF showed less efficacy compared to DEX or the DEX/TOF combination. Combined DEX and TOF exhibited an additive effect. Based on simulations,

a steroid-sparing potential may be achieved by combination therapy using a revised dosing regimen.

REFERENCES

1. McInnes IB, Schett G. Pathogenetic insights from the treatment of rheumatoid arthritis. Lancet. 2017;389(10086):2328–37.
2. Smolen JS, Aletaha D, McInnes IB. Rheumatoid arthritis. Lancet. 2016;388(10055):2023–38.
3. Burmester GR, Pope JE. Novel treatment strategies in rheumatoid arthritis. Lancet. 2017;389(10086):2338–48.
4. Coutinho AE, Chapman KE. The anti-inflammatory and immunosuppressive effects of glucocorticoids, recent developments and mechanistic insights. Mol Cell Endocrinol. 2011;335(1):2–13.
5. Scherholz ML, Schlesinger N. Androulakis IP. Advanced Drug Delivery Reviews: Chronopharmacology of glucocorticoids; 2019.
6. Cato AC, Nestl A, Mink S. Rapid actions of steroid receptors in cellular signaling pathways. Science's STKE : Signal Transduction Knowledge Environment. 2002;2002(138):re9.
7. Scott DL, Stevenson MD. Treating active rheumatoid arthritis with Janus kinase inhibitors. Lancet. 2017;390(10093):431–2.
8. Fleischmann R. Tofacitinib in the treatment of active rheumatoid arthritis in adults. Immunotherapy. 2018;10(1):39–56.
9. Dowty ME, Jesson MI, Ghosh S, Lee J, Meyer DM, Krishnaswami S, et al. Preclinical to clinical translation of tofacitinib, a Janus kinase inhibitor, in rheumatoid arthritis. J Pharmacol Exp Ther. 2014;348(1):165–73.
10. Milici AJ, Kudlacz EM, Zwillich S, Changelian P. Cartilage preservation by inhibition of Janus kinase 3 in two rodent models of rheumatoid arthritis. Arthritis Res Ther. 2008;10(1):R14.
11. LaBranche TP, Jesson MI, Radi ZA, Storer CE, Guzova JA, Bonar SL, et al. JAK inhibition with tofacitinib suppresses arthritic joint structural damage through decreased RANKL production. Arthritis Rheum. 2012;64(11):3531–42.
12. Earp JC, Pyszczynski NA, Molano DS, Jusko WJ. Pharmacokinetics of dexamethasone in a rat model of rheumatoid arthritis. Biopharm Drug Dispos. 2008;29(6):366–72.
13. Song D, DuBois DC, Almon RR, Jusko WJ. Modeling sex differences in anti-inflammatory effects of dexamethasone in arthritic rats. Pharm Res. 2018;35(11):203.
14. Kumar V, Dhiman V, Giri KK, Sharma K, Zainuddin M, Mullangi R. Development and validation of a RP-HPLC method for the quantitation of tofacitinib in rat plasma and its application to a pharmacokinetic study. Biomed Chromatogr. 2015;29(9):1325–9.
15. Sharma K, Giri K, Dhiman V, Dixit A, Zainuddin M, Mullangi R. A validated LC-MS/MS assay for simultaneous quantification of methotrexate and tofacitinib in rat plasma: application to a pharmacokinetic study. Biomed Chromatogr. 2015;29(5):722–32.
16. Dixit A, Mallurwar SR, Sulochana SP, Zainuddin M, Mullangi R. Determination of tofacitinib in mice whole blood on dried blood spots using LC-ESI-MS/MS: application to pharmacokinetic study in mice. Drug Research. 2019;69(06):330–6.
17. Dowty ME, Lin J, Ryder TF, Wang W, Walker GS, Vaz A, et al. The pharmacokinetics, metabolism, and clearance mechanisms

of tofacitinib, a Janus kinase inhibitor, in humans. Drug Metab Dispos. 2014;42(4):759–73.

18. Krishnaswami S, Boy M, Chow V, Chan G. Safety, tolerability, and pharmacokinetics of single oral doses of tofacitinib, a Janus kinase inhibitor, in healthy volunteers. Clin Pharm Drug Dev. 2015;4(2):83–8.

19. Cao Y, Jusko WJ. Applications of minimal physiologically-based pharmacokinetic models. J Pharmacokinet Pharmacodyn. 2012;39(6):711–23.

20. Davies B, Morris T. Physiological parameters in laboratory animals and humans. Pharm Res. 1993;10(7):1093–5.

21. Kawai R, Mathew D, Tanaka C, Rowland M. Physiologically based pharmacokinetics of cyclosporine A: extension to tissue distribution kinetics in rats and scale-up to human. J Pharmacol Exp Ther. 1998;287(2):457–68.

22. Shah DK, Betts AM. Towards a platform PBPK model to characterize the plasma and tissue disposition of monoclonal antibodies in preclinical species and human. J Pharmacokinet Pharmacodyn. 2012;39(1):67–86.

23. Gupta K, Stock T, Wang R, Alvey C, Choo H, Krishnaswami S. A phase 1 study to estimate the absolute bioavailability of tofacitinib (CP-690,550) in healthy subjects. J Clin Pharmacol. 2001;51:1348.

24. Li X, DuBois DC, Song D, Almon RR, Jusko WJ, Chen X. Modeling combined immunosuppressive and anti-inflammatory effects of dexamethasone and naproxen in rats predicts the steroid-sparing potential of naproxen. Drug Metab Dispos. 2017;45(7):834–45.

25. Dayneka NL, Garg V, Jusko WJ. Comparison of four basic models of indirect pharmacodynamic responses. J Pharmacokinet Biopharm. 1993;21(4):457–78.

26. Earp J, Krzyzanski W, Chakraborty A, Zamacona MK, Jusko WJ. Assessment of drug interactions relevant to pharmacodynamic indirect response models. J Pharmacokinet Pharmacodyn. 2004;31(5):345–80.

27. D'Argenio D, Schumitzky A, Wang X. Adapt 5 user's guide: pharmacokinetics/pharmacodynamic systems analysis software. BMSR: University of Southern California; 2009.

28. Boxenbaum H. Interspecies scaling, allometry, physiological time, and the ground plan of pharmacokinetics. J Pharmacokinet Biopharm. 1982;10(2):201–27.

29. Tang H, Mayersohn M. A novel model for prediction of human drug clearance by allometric scaling. Drug Metab Dispos. 2005;33(9):1297–303.

30. Losel R, Wehling M. Nongenomic actions of steroid hormones. Nat Rev Mol Cell Biol. 2003;4(1):46–56.

31. Suzuki M, Tse S, Hirai M, Kurebayashi Y. Application of physiologically-based pharmacokinetic modeling for the prediction of tofacitinib exposure in japanese. Kobe J Med Sci. 2017;62(6):E150–E61.

32. Ma G, Xie R, Strober B, Langley R, Ito K, Krishnaswami S, et al. Pharmacokinetic characteristics of tofacitinib in adult patients with moderate to severe chronic plaque psoriasis. Clin Pharm Drug Dev. 2018;7(6):587–96.

33. Wang X, Krishnaswami S, Tse S, Lin J, Dowty M, Menon S, et al. Inflammation and cytochrome P450 mediated metabolism of tofacitinib. ASCPT Annual Meeting. 2016.

34. English J, Chakraborty J, Marks V. The metabolism of dexamethasone in the rat–effect of phenytoin. J Steroid Biochem. 1975;6(1):65–8.

35. Tomlinson ES, Lewis DF, Maggs JL, Kroemer HK, Park BK, Back DJ. In vitro metabolism of dexamethasone (DEX) in human liver and kidney: the involvement of CYP3A4 and CYP17 (17,20 LYASE) and molecular modelling studies. Biochem Pharmacol. 1997;54(5):605–11.

36. Gupta P, Alvey C, Wang R, Dowty ME, Fahmi OA, Walsky RL, et al. Lack of effect of tofacitinib (CP-690,550) on the pharmacokinetics of the CYP3A4 substrate midazolam in healthy volunteers: confirmation of in vitro data. Br J Clin Pharmacol. 2012;74(1):109–15.

37. Pascussi JM, Drocourt L, Fabre JM, Maurel P, Vilarem MJ. Dexamethasone induces pregnane X receptor and retinoid X receptor-alpha expression in human hepatocytes: synergistic increase of CYP3A4 induction by pregnane X receptor activators. Mol Pharmacol. 2000;58(2):361–72.

38. Teo YL, Saetaew M, Chanthawong S, Yap YS, Chan EC, Ho HK, et al. Effect of CYP3A4 inducer dexamethasone on hepatotoxicity of lapatinib: clinical and in vitro evidence. Breast Cancer Res Treat. 2012;133(2):703–11.

39. Lamba M, Hutmacher MM, Furst DE, Dikranian A, Dowty ME, Conrado D, et al. Model-informed development and registration of a once-daily regimen of extended-release tofacitinib. Clin Pharmacol Ther. 2017;101(6):745–53.

40. Fleischmann R, Kremer J, Tanaka Y, Gruben D, Kanik K, Koncz T, et al. Efficacy and safety of tofacitinib in patients with active rheumatoid arthritis: review of key phase 2 studies. Int J Rheum Dis. 2016;19(12):1216–25.

41. Fleischmann R, Mysler E, Hall S, Kivitz AJ, Moots RJ, Luo Z, et al. Investigators OS. Efficacy and safety of tofacitinib monotherapy, tofacitinib with methotrexate, and adalimumab with methotrexate in patients with rheumatoid arthritis (ORAL strategy): a phase 3b/4, double-blind, head-to-head, randomised controlled trial. Lancet. 2017;390(10093):457–68.